

Functional model of a simplified clarinet

Stephen E. Stewart and William J. Strong

Department of Physics and Astronomy, Brigham Young University, Provo, Utah 84602
(Received 13 July 1979; accepted for publication 5 April 1980)

A functional model of a simplified clarinet has been developed and implemented on a digital computer. The simplified clarinet consists of a standard clarinet mouthpiece and reed attached to a straight cylindrical tube. In the model, the tube and mouthpiece are represented by a lumped element approximation to a transmission line and the reed is represented as a nonuniform bar, clamped at one end. Differential equations for the system are solved numerically on a digital computer to obtain pressures and volume velocities of the air in the tube and mouthpiece, and positions of the reed at successive time increments. The model exhibits self-sustained oscillations, threshold blowing pressures, frequency shifts, and spectra of mouthpiece and radiated pressures which are similar to those of an actual simplified clarinet. A previously unreported dependence of volume velocity in the reed aperture on the initial or rest opening of the aperture was also found.

PACS numbers: 43.75.Ef, 43.85.Ta

INTRODUCTION

Some of the earliest studies on the physics of vibrations and wave motion were precipitated by an interest in understanding musical instruments and musical tones. Yet, science has been able to offer little support to the design and fabrication of musical instruments. This has not been entirely the fault of the musical instrument craftsmen who tend to view their work as an art form. It is largely because the physics of musical instruments and their tone production has not been sufficiently understood for it to be much help in designing or building instruments. There is gathering evidence that this picture is beginning to change.

Research has been done on many different musical instruments including the mechanical reed woodwinds (e.g., clarinet, oboe, and bassoon) which form an interesting class of instruments to study. For historical (to about 1960) examples of the research on mechanical reed woodwinds the reader is referred to the work of Helmholtz,¹ Miller,² Bouasse,³ Aschoff,⁴ McGinnis and Gallagher,⁵ and Morse.⁶ More recently Benade has provided an overview of the physics of woodwinds,⁷ considerations of woodwind bores,⁸ and woodwind tone hole theory.⁹

The first really successful mathematical theory for small oscillations in a clarinet is due to Backus. In a paper¹⁰ published in 1963 he treated the clarinet reed as a damped, simple harmonic oscillator driven by sinusoidal oscillations of the air column. He was able to derive expressions for threshold blowing pressure and frequency shift in the tone due to a damping-induced phase shift in the reed vibrations relative to the mouthpiece pressure. The excellent agreement of his theory with experiment clearly established the importance of reed damping in clarinet tone production, and many of his measurements, particularly those for volume velocity in the reed aperture as a function of pressure difference and reed opening, have had a basic role in nearly all of the work done on the clarinet since. In a book on woodwind instruments published in 1969, Nederveen¹¹ elaborated on Backus' work, but his main

emphasis was on instrument bores and tone holes.

In 1968, Benade and Gans,¹² inspired by Bouasse's work, outlined a qualitative, nonlinear theory for oscillations in wind instruments. Then, in 1971, Worman¹³ filled out the theory with mathematical details for clarinet-like systems. Worman followed Backus in considering the clarinet reed as a damped, simple harmonic oscillator, but he considered nonlinear air flow through the reed aperture and was able to calculate spectra for the clarinet which agree well with measured spectra. However, because of the complexity of the mathematics involved, Worman chose to work with a model of a tube that had only a single resonance and a single antiresonance. In 1978, Schumacher¹⁴ applied an integral equation approach to Worman's equation and, with the help of some powerful computer programs, was able to work out solutions for a tube with three resonances and two antiresonances. Recently, Schumacher¹⁵ indicated that he had pushed the solutions even further and was able to do calculations for fairly realistic clarinet tubes. In two papers published in 1978 and 1979, Fletcher^{16,17} discusses nonlinearities in some musical instruments. In the first, he describes mode locking, where instruments with slightly inharmonic resonances generate strictly harmonically related partials. In the second, he gives a qualitative discussion of harmonic generation in wind instruments.

The work done during the last two decades represents significant advances in understanding the physics of tone production, but it is clear that there is more work that needs to be done. A general restriction observed in almost all research on the clarinet to date has been to treat only small- and medium-amplitude reed vibrations in which the reed does not beat against the mouthpiece. Schumacher did try to incorporate the beating reed in his calculations, but he did it in a nonphysical way. The research has also been restricted primarily to steady-state oscillations. One would ultimately like to study the details of loud tone production in the clarinet where the reed does beat and also to consider transient behavior. It has also been a consistent practice to treat the reed as merely a damped simple harmonic oscillator,

a single mass on a spring. One might ask, however, what the effect is of different placements of the player's lip along the reed and what is the detailed way in which necessary damping is supplied to the entire reed by the player's lip? Also, what is the instantaneous shape of the reed aperture and how are the aperture resistance and inductance affected by the shape?

It is with the aim of shedding some light on these and other questions that we have created a functional model, on a digital computer, of a simplified clarinet. A functional model should duplicate as closely as possible the functioning of the physical system it represents. Every physical quantity in the real system should have its counterpart in the model. This essential nature of functional modeling makes it quite useful in investigating systems with complicated interactions such as found in the clarinet. It is very unlikely that a functional model will behave like the real system unless it includes all of the important features of the real system. Thus one is often led to uncover subtle but important features of the system which may have previously been overlooked. And usually, the precise way in which the behavior of the model differs from that of the real system is a strong clue as to what may not have been correctly incorporated in the model. Once the model has been correctly created, it provides a means to more easily determine the effect of variations in the system since the software of the model is generally much easier to modify than the hardware of the system. And finally, there are often quantities which are very difficult to measure in the real system which are readily accessible in the model.

Our model is not the first attempt at creating a functional model of a clarinet. Higbee and Turley¹⁸ created a functional model in which they approximated the reed as a simple mass on a spring and the cylindrical tube as a lossy delay line. The lossy delay line representation treats each section of tube in terms of reflection coefficients at its ends with propagation delay and loss included explicitly. In spite of the rather gross approximations involved in their model, they were able to demonstrate self-sustained oscillations, a threshold blowing pressure in the neighborhood of that found by Backus,¹⁰ and a mouthpiece waveform roughly like those of real clarinets. There may have been other attempts at functional clarinet modeling, but nothing more could be found in the literature on the subject.

We must emphasize that our model is not of a real clarinet. We have tried to include all of the important features of the reed and mouthpiece of the clarinet, but we have greatly simplified the rest of the model by considering the mouthpiece to be attached to a simple cylindrical tube without tone holes or flare. The inclusion of tone holes and flare in the tube represents an additional task, probably of equal magnitude with that of the original modeling of the reed, mouthpiece, and simple tube, and must remain for later work. The current model is applicable to clarinet research because of the clarinet-like features of the reed and mouthpiece, but it must be considerably extended and refined before it can be considered as a model of a real clarinet.

This paper consists of two main sections. In the first, the model is described and the step-by-step development and implementation of the model on a digital computer is outlined. The second section details the results obtained with the model and how they relate to experimental and theoretical work previously done by others. Finally, a short summary indicates what might be done next in investigating tone production in mechanical reed woodwinds.

I. DESCRIPTION OF THE FUNCTIONAL MODEL

In this section we describe the specific representations used for the tube and reed in the model. We explain why the particular representations were chosen and briefly how they were incorporated into the computer simulation. We also describe the coupling between the air column vibrations and the reed motion.

A. Representation of the tube

Figure 1 shows a schematic representation of a simplified clarinet which is the object of the functional modeling. The simplified clarinet consists of a cylindrical tube (inside diameter of 1.50 cm and length of 43.5 cm) to which is attached a clarinet mouthpiece (length of 3.5 cm and variable cross-sectional area). The cross-sectional area in the mouthpiece varies from 0.064 to 1.762 cm² over its length when the reed is closed. The mouthpiece has a volume of 2.965 cm³ and an "equivalent cylindrical length" of 1.68 cm.

Considerable direction for the initial formulation of the current model of the clarinet bore came from Flanagan's vocal tract model.^{19,20} In that model the vocal tract is represented as a lumped element approximation to a transmission line. The transmission line approach for the clarinet tube seemed more desirable than the lossy delay line because it could accommodate tone holes and flare in the tube more easily, although these complications have been left out of the current model.

Flanagan²¹ gives an analogous electrical circuit for a section of hard-walled cylindrical tube as shown in the center of the circuit at the bottom of Fig. 1. He gives derivations for the analogous inductance and capacitance in the circuit representing the per unit length inertia L and compliance C of the air in the tube and also for the analogous resistance R and conductance G in the circuit representing the viscous and heat conduction losses in the tube. The expressions for these quantities (shown

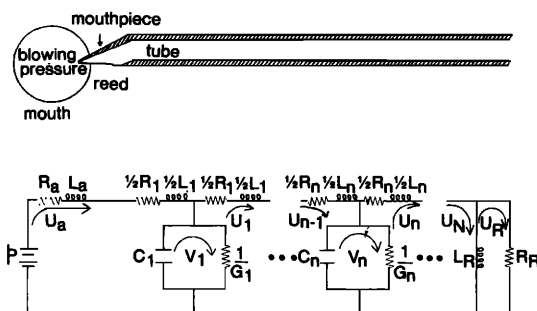


FIG. 1. Schematic representation of a simplified clarinet (top) and an equivalent circuit for it (bottom).

with subscripts in Fig. 1) are

$$L = \rho/A, C = A/\rho c^2, R = (S/A^2)(\omega\rho\mu/2)^{1/2} \quad (1)$$

and

$$G = (S/\rho c^2)(\eta - 1)(\lambda/2c_p\rho)^{1/2},$$

where ρ is the density of air, A is the cross-sectional area of the tube, c is the speed of sound in air, S is the circumference of the tube, μ is the coefficient of viscosity of air, λ is the coefficient of heat conduction, η is the adiabatic constant, and c_p is the specific heat of air at constant pressure. The radiation load in Flanagan's model is that for a piston in an infinite baffle which is adequate for sound radiating from the mouth, but for the clarinet the load on a piston in the end of a long tube is more appropriate. Beranek²² gives values for an equivalent parallel combination of resistance R_R and inductance L_R for this radiation load as

$$R_R = 0.479\rho c/a^2 \quad \text{and} \quad L_R = 0.1952\rho/a, \quad (2)$$

where a is the radius of the tube. The above expressions are only valid when $ka < 0.5$ which is not true for the higher harmonics in the clarinet, but is adequate for the purpose at hand.

The pressure fluctuations in the mouthpiece end of the tube act on the reed to drive it. The motion of the reed changes the size of the reed aperture which opens to allow more volume flow into the tube or closes to shut off the flow. In the analogous electrical circuit, the approximately constant blowing pressure p provided by the player's lungs is provided by a battery which acts through the variable resistance R_a and inductance L_a of the reed aperture to give the volume velocity U_a into the tube as shown in the circuit at the bottom of Fig. 1. Application of Kirchoff's circuit laws gives the integro-differential equations which relate the volume velocities (current) U and V in each section of the circuit. These equations are

$$\begin{aligned} p - R_a U_a - L_a \frac{dU_a}{dt} - \frac{1}{2} R_1 U_a - \frac{1}{2} L_1 \frac{dU_a}{dt} - \frac{1}{C_1} \\ \times \int_0^t (U_a - V_1) dt = 0, \\ \frac{1}{C_1} \int_0^t (U_a - V_1) dt - \frac{1}{G_1} (V_1 - U_1) = 0, \\ \vdots \\ \frac{1}{G_n} (V_n - U_n) - \frac{1}{2} (R_n + R_{n+1}) U_n - \frac{1}{2} (L_n + L_{n+1}) \frac{dU_n}{dt} \\ - \frac{1}{C_{n+1}} \int_0^t (U_n - V_{n+1}) dt = 0, \\ \frac{1}{C_{n+1}} \int_0^t (U_n - V_{n+1}) dt - \frac{1}{G_{n+1}} (V_{n+1} - U_{n+1}) = 0, \\ \vdots \\ \frac{1}{G_N} (V_N - U_N) - \frac{1}{2} R_N U_N - \frac{1}{2} L_N \frac{dU_N}{dt} - L_R \left(\frac{dU_N}{dt} - \frac{dU_R}{dt} \right) = 0, \\ L_R \left(\frac{dU_N}{dt} - \frac{dU_R}{dt} \right) - R_R U_R = 0. \end{aligned} \quad (3)$$

This set of simultaneous equations is approximated by finite difference equations and solved numerically by Euler's method to get the volume velocity in each section of tube. The pressure in the n th section is given by $p_n = (V_n - U_n)/G_n$ and the radiated pressure is $p_R = R_R U_R$. It was found that the numerical solution to the set of difference equations remained stable for larger step sizes if the pressure across the capacitor is left as an integral rather than substituting in the pressure and its derivative in the equations and solving for the volume velocities and pressures simultaneously. Also, more sophisticated numerical methods, such as the Range-Kutta methods, proved to be not as stable as Euler's method.

Since the tube is represented by a ladder network, it exhibits a cutoff frequency and the filtering of higher frequencies that occurs makes each section appear to ring after abrupt changes of the volume velocity. The "ringing" is due to the lumped element approximation and can be made negligibly small by decreasing the length of each section while increasing the number of sections to keep the total length of the tube constant. The effect of decreasing the section length is to decrease the size of the lumped elements, thereby more closely approximating the continuous case. A standard criterion for the length of individual sections is derived²³ as $l \ll \lambda/2\pi$, where λ is the wavelength of the highest frequency expected in the tube. The current model incorporates 0.25-cm sections in the straight portion of the tube where the cross-sectional area is constant and 0.1-cm sections in the tapered mouthpiece.

Initially the tube was programmed with values for the resistive elements that represented an average over the frequencies expected in the tube, as is commonly done in speech simulation, and the frequency dependence of the tube losses was not incorporated. The tube had a constant loss for all frequencies which was too high for the low frequencies and too low for the high frequencies. As might be expected, this showed up in the spectra of the mouthpiece and radiated pressure waveforms. Apparently, constant average losses are adequate in a vocal tract model because the vocal tract resonances are not ordinarily harmonically related, the vocal tract resonances are more heavily damped than those of a clarinet, and the vocal cords vibrate with a fundamental lower than resonances of the tract, all of which result in weak coupling between the vocal cords and tract. In the clarinet, however, the reed is very strongly affected by the air column vibrations and the high frequencies also couple to the reed more strongly since the natural frequency of the reed is about an order of magnitude higher than the fundamental of the clarinet. In order to incorporate frequency dependent losses in our model, different expressions for the viscous and heat conduction losses had to be derived. The explicit appearance of frequency in the expressions given by Flanagan is incompatible with a time-evolving system. The viscous loss represents at least two-thirds of the total loss so it was first to be considered.

The drag force in the k th section of tube at the N th time interval was derived as (see Appendix)

$$F_k = (\rho\mu/\pi h)^{1/2} \sum_{n=1}^N (u_{N-n}^{(k)} - u_{N-1-n}^{(k)})n^{-1/2}, \quad (4)$$

where $u_n^{(k)}$ is the n th sample of the particle velocity of the air in the k th section of tube and h is the interval size (i.e., time increment for calculations). It is seen that a large number of previous samples of velocity need to be stored and a convolution sum performed for each section of tube. Because of limited core space in the computer and considerations of calculation times, it was not possible to incorporate this frequency-dependent loss correctly in each section. As a compromise it was decided to concentrate the loss for the entire tube in just one section and to use a sum extending to 1000 terms for that loss. Since truncation of the sum at 1000 terms produces a slight error in the loss, a portion of the original average loss was retained to make the Q of the tube about right for the fundamental frequency. The lumped, frequency-dependent loss was incorporated in the model in the form of a variable battery placed in series in the last section of tube immediately before the radiation load. The "voltage" of the battery is given by

$$LSA^{-2}(\rho\mu/\pi h)^{1/2} \sum_{n=1}^{1000} (U_{-n} - U_{-n-1})n^{-1/2}, \quad (5)$$

where L is the length of the tube, S is the circumference, A is the cross-sectional area, and U_{-n} is the n th previous sample of the volume velocity.

Because of the huge computational and storage costs of the proper inclusion of the frequency-dependent viscous loss, and because the inclusion of it in the manner described above did achieve the desired effect of reducing the power in the high frequencies relative to that in the low frequencies, it was decided not to attempt anything similar with the heat conduction losses. The heat conduction losses remained as constant average losses for all frequencies. For future work with the model it might be well to include the heat conduction losses simply as a fraction of the viscous losses.

B. Representation of the reed

As pointed out earlier, in most of the mathematical theories developed for the clarinet to date, the reed has been modeled as a simple harmonic oscillator. This approximation deserves some discussion. Some investigators had previously reported quite complicated motions in clarinet reeds,⁵ but more careful studies²⁴ have not found such motions. The clarinet reed oscillates at a frequency below that of its fundamental mode so that all points on the reed move in phase, but with increasing amplitude toward the tip. Furthermore, the deflection of the tip of a free clarinet reed clamped at its base is a linear function of applied force. One is naturally led to modeling the clarinet reed as a mass on a spring with an effective mass, spring constant, and damping to give it the same properties of motion as the tip of an actual reed. Such a representation certainly simplifies the programming and calculations, but it is not adequate to capture all of the phenomena relevant to the interaction of the reed with the mouthpiece and the player's lip. As the reed on a clarinet mouthpiece moves toward closure of the reed aperture it must bend against the

curved lay of the mouthpiece. As it does so, the effective mass and stiffness of the remaining portion of the reed, which is still free to move, changes. This effect would have to be added explicitly to a spring-mass model, whereas a more realistic model would probably incorporate it automatically. The effect of position of the player's lip along the reed also falls in the same category.

The reed in our model is represented as a damped, driven, nonuniform bar clamped at one end. The differential equation for transverse vibrations of a bar can be found in many acoustics textbooks.²⁴ With a driving force and damping added, and taking into account the nonuniform thickness, the equation becomes

$$\rho A \partial^2 y / \partial t^2 + R \partial y / \partial t = \partial^2 / \partial x^2 (YA \kappa^2 \partial^2 y / \partial x^2) + F, \quad (6)$$

where ρ is the mass density of the bar, A is its cross-sectional area, R is the damping per unit length, Y is its Young's modulus, κ is its radius of gyration, and F is the externally applied force per unit length. For a bar of rectangular cross section, $\kappa = b/(12)^{1/2}$, where b is the thickness of the bar. Both A and κ are functions of position for a clarinet reed and must be determined by measuring the thickness and width of the particular reed to be modeled, and Y and ρ must also be determined from the reed. For cane reeds, ρ is about 0.5 g/cm³ and Y is about 5×10^{10} dynes/cm² although these numbers may vary considerably from reed to reed. Integration of the bar equation for the static case gives a formula for determining Y from measured deflections under static loads. We determined the damping R by running the functional model of the reed by itself and adjusting R until about the same exponential decay was observed in the model as for a real reed (held in the hand to provide damping) when both were set in motion by an impulse. The force F is part of the coupling between the reed and the air column and will be discussed a little later. The boundary conditions to be satisfied by the equation at the ligature end which we assume to be clamped are $y=0$ and $\partial y / \partial x = 0$ and at the free end they are $\partial^2 y / \partial x^2 = 0$ and $\partial^3 y / \partial x^3 = 0$.

An implicit numerical method²⁶ was used to solve the reed equation. The differential equation was written as a difference equation for each 0.1 cm section of the reed where the derivatives with respect to position at the current time are written as the average of the derivatives at the previous time and the next time, i.e., $(\partial^4 y / \partial x^4)_t = \frac{1}{2} (\partial^4 y / \partial x^4)_{t+\Delta t} + \frac{1}{2} (\partial^4 y / \partial x^4)_{t-\Delta t}$. The resulting set of simultaneous equations for the displacements of the segments at the next time in terms of their displacements at the current and previous times was solved using a Gauss elimination procedure for five-diagonal systems. An explicit numerical method would have been more straightforward to use, but it was found to be stable only at sampling rates exceeding 5 MHz (5 million iterations for one second of real-time solution, i.e., a time step of 0.2 μ s). The implicit method, on the other hand, proved to be stable (but not too accurate) for rates as low as 2 kHz. The stability of the tube equations, however, requires that the entire model run at a sampling rate of 400 kHz or higher. The implicit method for the reed is quite accurate at this rate.

The rest position of the reed (the position to which the reed is brought when the player first bites down on it) could be set in two different ways. The reed could be clamped tightly against the lay at a point such as to give the desired opening or the position of the player's lip could be specified and a force applied at the point such as to push the reed up to the desired position. Once the reed has come to rest at the position, the force is replaced by a stop or limit so that the reed at that point is not allowed to move below the stop. The latter case is probably more realistic. In either case, however, damping due to the player's lip is added to the damping of the sections over a 1-cm length about the point specified for the position of the player's lip. The collision that occurs when any section of the reed strikes the mouthpiece or the lip is made inelastic by setting the velocity of that section to zero and holding it there as long as it tends to move into the mouthpiece or lip. Stroboscopic observations of an actual vibrating clarinet reed revealed very little, if any, bouncing of the reed on the lay which provides justification for treating collisions as inelastic.

C. Coupling between reed and air column

There is a mutual interaction between the position of the reed and the pressure fluctuations in the tube. The forces acting on the reed are the force of the blowing pressure which always tends to close the reed aperture, the force of the oscillating pressure developed in the mouthpiece, and the Bernoulli force due to the movement of air across the inside surface of the reed. The blowing pressure, provided by the player's lungs, is taken to be constant. This may not be strictly true, but the fluctuation is small and we have neglected it in our current model. The pressure in the mouthpiece is developed as a consequence of the fluctuating volume flow of air through the reed aperture and the reflections of the resulting pressure waves from the ends of the tube. The Bernoulli pressure is calculated directly from the flow by $p_B = \frac{1}{2} \rho (U/A)^2$, where ρ is the density of the air, U is the volume velocity and A is the cross-sectional area through which the air flows. The Bernoulli pressure acts over the entire reed but it is only significant at the tip where A is small. Thus, the forces on the reed are determined ultimately by the volume flow and, for a given pressure difference across the reed, the volume flow is determined by the position of the reed. The volume flow through the reed aperture is really the coupling agent between the reed and the air column. It is very important for any model of the clarinet to accurately capture the dependence of the volume flow on the reed opening.

In our functional model the aperture volume flow for a given pressure difference across the reed is controlled by the variable aperture resistance and inductance which are determined by the position of the reed. First, we consider the resistance for steady flow. Backus gives an empirically determined expression for the volume flow for a clarinet reed aperture as a function of reed opening and pressure difference across the reed from which the aperture resistance could be determined. However, he did not include measurements for

very small openings and thus neglected the most significant effects of viscosity on the flow for very small openings. Van den Berg²⁷ gives the empirically determined equation

$$R = 12\mu d/lw^3 + 0.875\rho U/2(lw)^2 \quad (7)$$

for the acoustic resistance of a rectangular slit, where l , w , and d are the length, height, and depth respectively of the slit (lw is the area through which the air flows) and U is the volume velocity in the slit. The first term in Eq. (7) is due to viscosity and the second term is due to turbulence effects. However, the reed aperture is not exactly rectangular, and Backus found experimentally that volume flow for a given pressure is approximately proportional to the reed opening to the $\frac{4}{3}$ power instead of the first power as normally found for medium-height rectangular slits. This proved not to be a serious difficulty in the functional model. Since the reed was already divided into 0.1-cm sections for the purpose of the reed position calculation it was convenient to divide the aperture up into approximately rectangular pieces as shown in Fig. 2 and calculate a resistance in the form of Eq. (7) for each piece. The total aperture resistance is just the parallel combination of the resistances for the separate pieces. Since the tip of a clarinet mouthpiece represents a different geometry than that treated by Van den Berg, one might expect to find a different constant in front of the turbulence term in Eq. (7) for the case of the reed aperture. In fact, we found it necessary to use

$$R = 12\mu d/lw^3 + 1.5\rho U/2(lw)^2 \quad (8)$$

for the resistance in order to get volume flows in the range of those reported by Backus.

Calculating the inductance of the slit on the same basis did not work well. The fact that the wedge-shaped portions of the reed aperture are situated at about 90° to the main rectangular portion apparently has some consequence for the effective inertia of the air in the opening. For the aperture inductance we determined empirically from Backus' data that the inductance is given approximately by $L_a = 2.85 \times 10^{-3} w^{-1/2}$, where w is now the opening at the tip of the reed. We must point out that even though the volume flow does not all enter the mouthpiece at the tip (i.e., in the first 0.1-cm section), our model treats it that way. We do not feel that

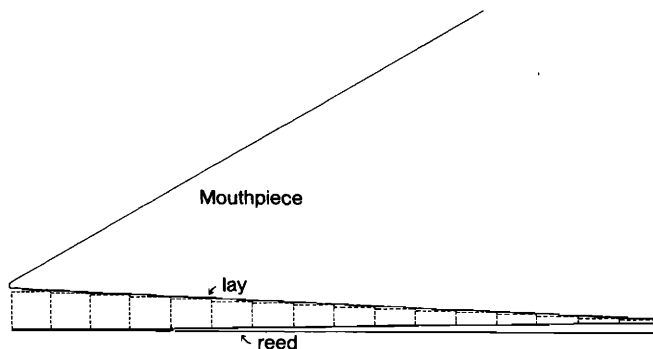


FIG. 2. The tip of a clarinet mouthpiece and reed showing the division (dashed lines) of the reed aperture into rectangular areas for the aperture resistance calculation.

this is a serious difficulty with the model, since the really significant effect of the increased air inertia in the aperture has been included in the model by using the aperture inductance given above.

II. RESULTS FROM THE FUNCTIONAL MODEL

The functional model described in Sec. I was programmed to run on a PDP-15 digital computer and runs at about 250 000 times real-time on that machine, that is, it takes the computer about 250 000 seconds, or over 67 hours to compute one second of vibration. The results that could be obtained from the model within a reasonable length of time have been somewhat limited by this poor real-time ratio. However, we have obtained enough results to be convinced that the model is a useful representation of an actual simplified clarinet and we have begun to gain some new insight into the functioning of a clarinet. In this section we will discuss results obtained from our model pertaining to volume flow in the reed aperture, threshold blowing pressure, frequency shifts in the tones, spectra of mouthpiece and radiated pressures, and attack transients. Because of the real-time ratio, curves illustrating many of these results had to be drawn from just a few (typically 6 to 8) calculated values.

A. Reed aperture volume flow

Backus determined that experimental data on the volume flow through a clarinet reed aperture for low pressures and medium openings are fit well by the relation¹⁰

$$U = 37p^{2/3}w^{4/3}, \quad (9)$$

where p is the pressure difference across the reed and w is the reed opening at the tip. Volume flows computed

from our model differ somewhat from this relationship. Figure 3 shows our results (solid lines) on volume flow as a function of reed opening plotted for three different blowing pressures. Equation (9) gives curves (dashed lines) with increasing slope everywhere, whereas our curves have slightly decreasing slope over part of their domain. The curvature is difficult to see in the figures, but it is real. The solid curves shown in Fig. 3 were all obtained for the same embouchure or rest (initial) opening of 0.08 cm. To obtain the curves, the vibrating reed in the model was simply "frozen" in place at different points in its vibratory cycle and, after the oscillations in the tube had died out, the reed position and volume velocity were printed. This would be virtually impossible to do on an actual clarinet.

Figure 4 shows curves for volume velocity versus reed opening which are obtained from the model for several different rest openings. These curves are all for the same blowing pressure of 40 mbar. A larger rest opening gives longer wedge-shaped openings along the sides of the mouthpiece which results in a greater volume velocity for a particular instantaneous reed opening and pressure. Experimentally, the functional dependence of volume flow on reed opening at a given pressure for a nonvibrating reed is obtained by varying the embouchure to get different reed openings at the tip. In order to compute volume flows from our model in a comparable manner we must move to successively lower curves in Fig. 4 to decrease the opening. The result for a particular pressure is a curve with increasing curvature everywhere as shown in Fig. 5. Here we have plotted volume velocity as a function of reed opening for pressures of 20, 40, and 60 mbar. Equation (9) is shown by dashed lines for the same pressures for com-

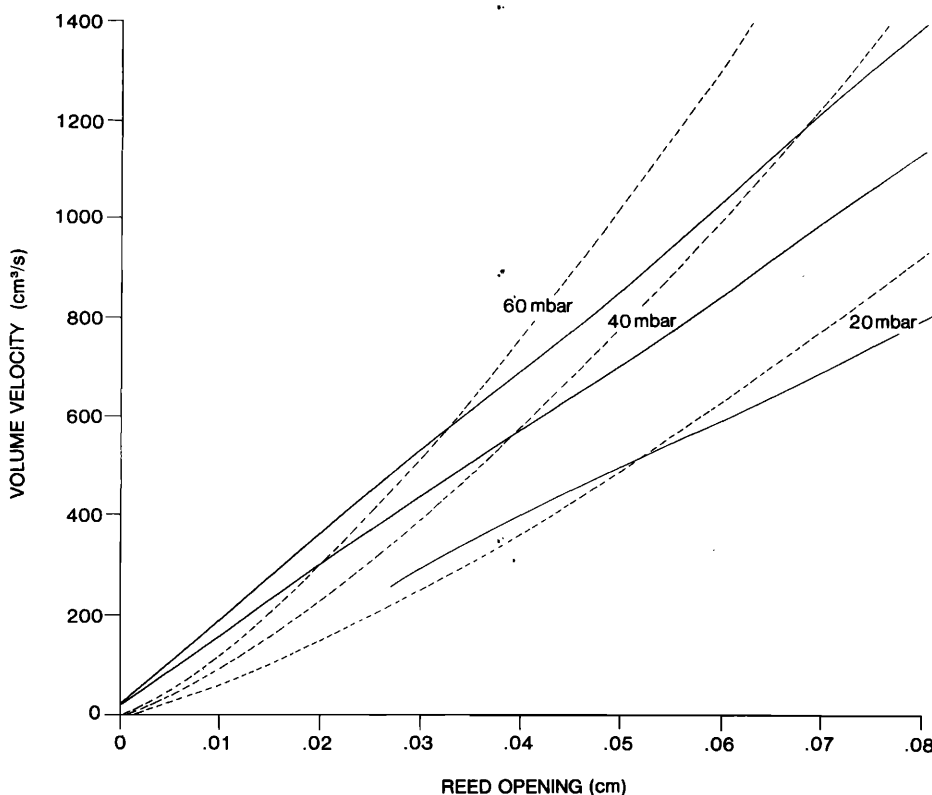


FIG. 3. Volume velocity in the reed aperture as a function of opening at the reed tip for three different blowing pressures. Results from the model for a rest opening of 0.08 cm are shown by the solid lines; Backus' empirically determined equation for reed aperture volume velocity [Eq. (9)] is shown by the dashed lines.

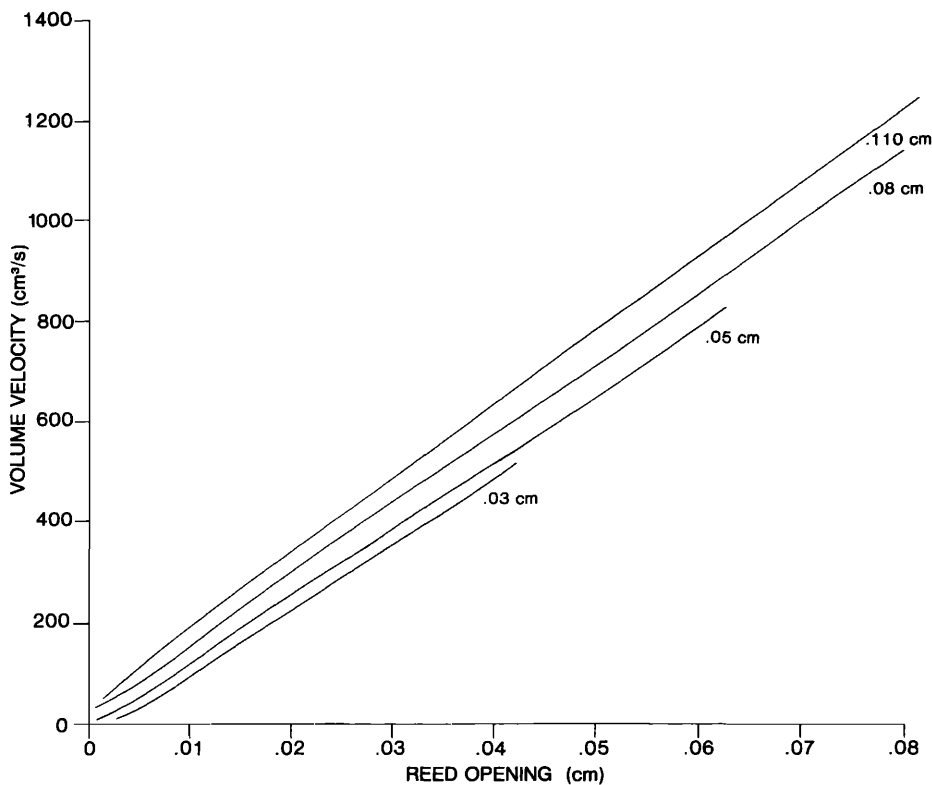


FIG. 4. Results from the clarinet model on volume velocity in the reed aperture as a function of opening at the reed tip at a blowing pressure of 40 mbar for four different rest openings.

parison. Our curves follow Eq. (9) more closely when aperture volume velocities are computed following Backus' experimental procedure, particularly for the medium-sized openings and lower pressures with which he dealt. We believe, however, that the functional relationship between volume velocity, reed opening, pressure, and rest opening which is illustrated in Figs. 3 and 4 is the more realistic for the clarinet under playing conditions. A clarinet player blows his instrument

with a set embouchure. And while he may change the embouchure, he does so only over a time which is long compared to the period of vibration of the reed.

B. Threshold blowing pressure

The determination of threshold blowing pressures was greatly hindered by the real-time ratio mentioned earlier. In an effort to find the threshold pressures more

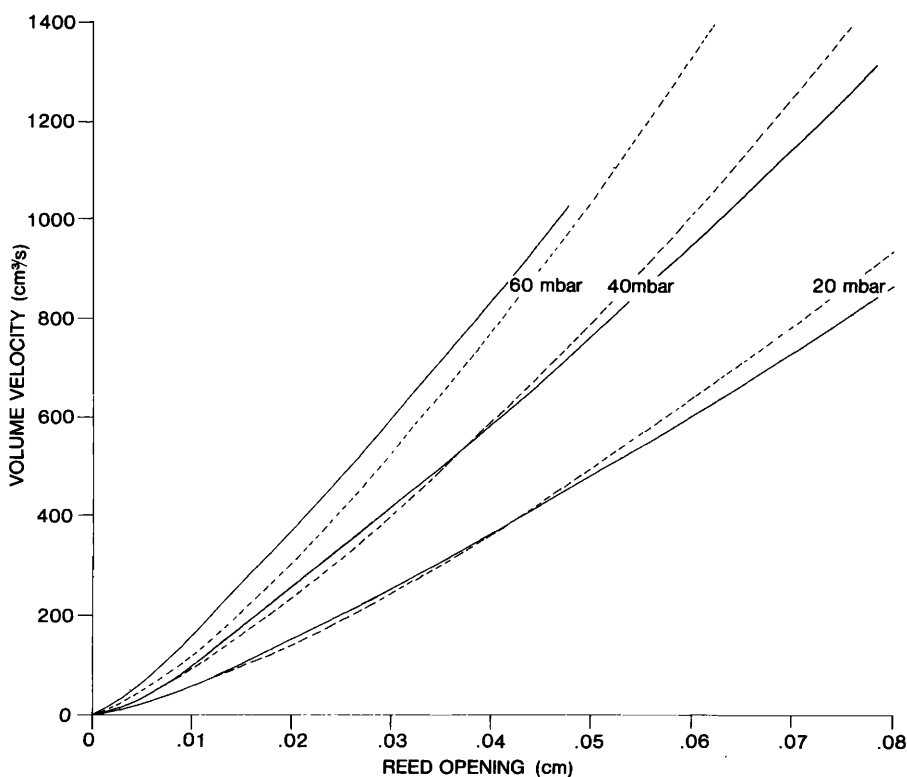


FIG. 5. Volume velocity in the reed aperture as a function of opening at the reed tip for three different blowing pressures. These curves (solid lines) were obtained by varying the rest opening. Equation (9) is shown by dashed lines.

quickly, we first computed steady flow (i.e., nonvibrating air column) volume velocities in our model as a function of initial reed (rest) opening and pressure difference across the reed. In this case the reed was allowed to move under the applied pressure and assume a new static equilibrium position. Our results are shown in Fig. 6 by the solid curves. Each curve is for a different rest (initial) opening of the reed aperture, the lower curves corresponding to tighter embouchures. As shown by the curves, the volume velocity first increases as the pressure difference increases, but then as the increased pressure pushes the reed closer to the lay, the flow begins to decrease. Finally the pressure difference becomes large enough to push the reed tightly against the lay and shut off the flow completely.

The curves of Fig. 6 exhibit all of the characteristics described by Benade²⁸ such as their asymmetry and maxima at larger pressure differences for larger rest openings. A curve from Worman¹³ based on Backus' results is shown in Fig. 6 as a broken line. Worman does not indicate what the rest opening was in determining this curve. He gives the effective stiffness per unit area of the reed used as 1.25×10^6 dynes/cm². The exact values of the volume velocity depend heavily on the stiffness of the reed employed. An effective stiffness per unit area can be calculated for a reed by dividing the pressure difference across the reed by the resulting deflection of the tip of the reed. The reed that we used for all of the computations described in this paper was found to have an effective stiffness of about 1.3×10^6 dynes/cm². The stiffness obtained by the method just described varies somewhat according to how much of the reed is in contact with the lay of the mouthpiece.

As Benade points out, self-sustained oscillations in

the clarinet can occur only when it is operating on the downward sloping portion of the curves in Fig. 6 where an increase in pressure in the mouthpiece (decrease in pressure difference) results in increased flow through the reed aperture. Clearly, for a particular rest opening, the blowing pressure would have to be greater than the pressure at the peak of the corresponding curve in Fig. 6 for this condition to be met. The peaks are joined by a dashed line and it is seen that the threshold blowing pressure should increase with increasing rest opening. Not only must the blowing pressure be to the right of the dashed line in Fig. 6, it must be far enough to the right so that the power injected into the tube when the reed opens more, due to an increase in mouthpiece pressure, is greater than that lost by a pressure wave in traveling to the end of the tube and back twice. By running our model with blowing pressures lying somewhat to the right of the dashed line in Fig. 6, we were able to determine that the threshold blowing pressure must lie within the shaded region shown in Fig. 7. To determine the threshold blowing pressure more exactly would take considerably more computer time. As a further complication, we also found that the threshold blowing pressure depends somewhat on the damping of the reed. If the reed is heavily damped, the threshold blowing pressure is higher by a few millibars. This seems to be contrary to the findings of Backus. However, we have not yet been able to determine whether the large amount of damping needed to change the threshold pressure significantly is actually physically realizable. It is a little hard to compare our results with Backus' data because he gives the pressure as a function of average reed opening and ours are as a function of rest opening, but the agreement is probably quite reasonable. If we consider Backus' average reed open-

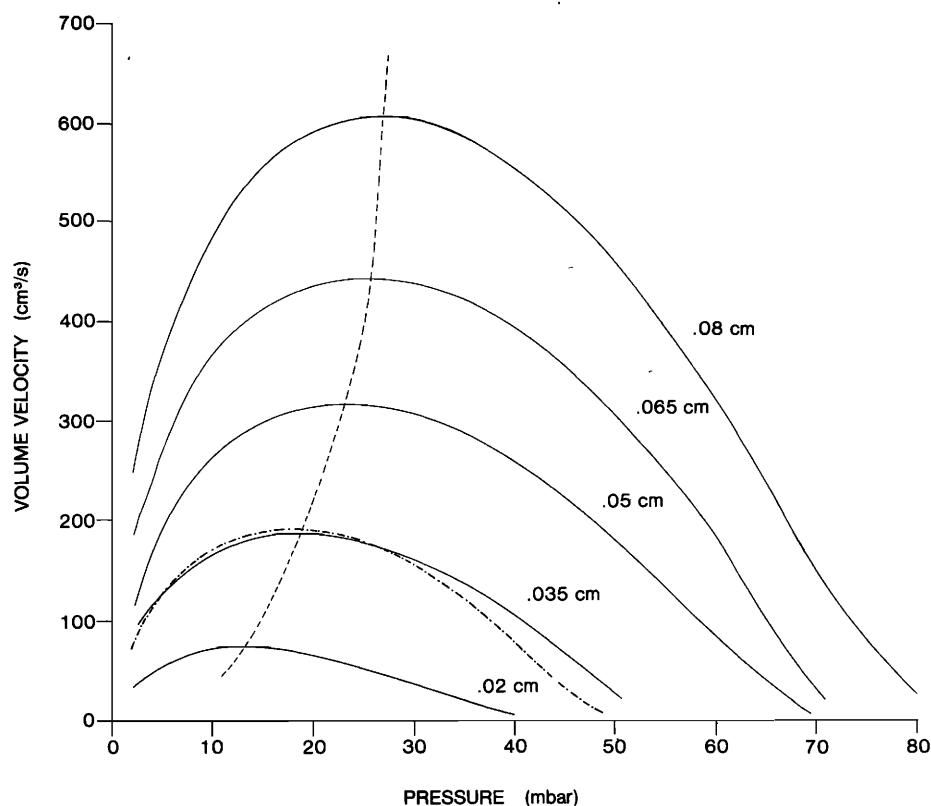


FIG. 6. Volume velocity in the clarinet model as a function of pressure difference across the reed for five different rest openings. The dashed line is drawn through the maxima of the curves. The broken line is from Worman.

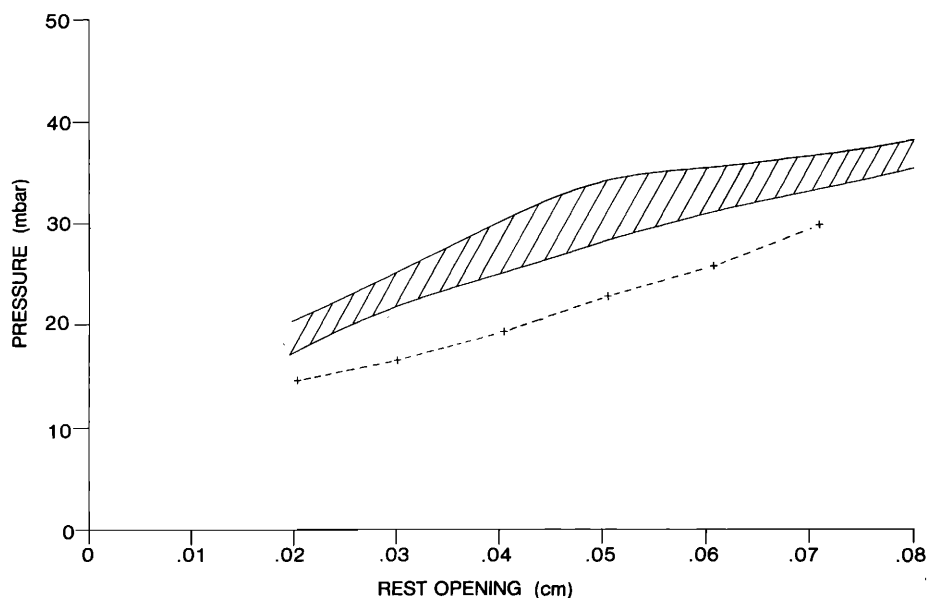


FIG. 7. Threshold blowing pressure for the clarinet model as a function of rest opening. Our computed threshold pressures fall within the shaded region. The crosses joined by a dashed line show Backus' data.

ing to be about one-half of our rest opening, then Backus' data would fall at the crosses joined by the dashed line in Fig. 7. Our pressures are somewhat higher than his, but that is probably due to a difference in reed stiffness or Q of the tube. In reviewing the manuscript, Benade suggested that we should check the insensitivity of the model to changes in residual reed aperture such as might result from slipping the reed down the mouthpiece one or two millimeters. We feel that the model would exhibit such insensitivity, but it was impractical for us to rerun the model to check this point.

Since threshold blowing pressure also depends upon the Q of the tube, we felt that it was important that our model exhibit the proper Q . Here again we were hindered by the real-time ratio. Most determinations of the Q of the tube involve driving the air in the tube with a sinusoid over a range of frequencies and measuring bandwidths from which Q can be determined. Any method which requires steady state oscillations for many different frequencies would have taken weeks of computer time to run on the model. We found, however, that the Q of a strictly cylindrical tube could be determined by a much faster method.

The tube is driven at the mouthpiece end by a constant amplitude volume velocity sinusoid. If p_0 is the pressure amplitude generated by the driver and E is the ratio of the reflected pressure amplitude to p_0 , then, after one round-trip transit time for the wave we have the pressure amplitude in the mouthpiece given by

$$p_1 = p_0(1 + 2E) \quad (10)$$

if the driver is at a resonance frequency. At resonance, the input pressure and the reflected pressure will be in phase and p_1 will be at a maximum. The resonance frequency must still be found, but one has the advantage of not having to wait for the oscillations to reach steady state at each frequency. The amplitudes p_1 and p_0 are obtained from the model at a resonance frequency and Eq. (10) is solved for E . By manipulating several equa-

tions found in Benade⁸ we find that the Q for a cylindrical tube is given by

$$Q = (-\omega l/c)(\ln E)^{-1} \approx (\omega l/c)(1 - E)^{-1}, \quad (11)$$

where ω is the angular frequency, c is sound speed, and l is the length of the tube.

Since neither Eq. (10) nor (11) applies to a tapered tube we could only determine the Q of our model by replacing the tapered mouthpiece with an equivalent length of cylindrical tube. By applying the method described above to such a tube with the taper removed, we were able to determine that the losses, as included in our model, give approximately the right Q at frequencies of the first few normal modes.

C. Frequency shifts

Of great importance to clarinetists is the slight but definite control which they can exercise on the playing frequency of their instrument by varying lip pressure and position on the reed. This effect was first described mathematically for small vibrations by Backus.¹⁰ He was able to show that the fractional frequency shift in the tone depends on the damping on the reed and the Q of the instrument as well as the average reed opening. The reed damping induces a phase shift in the reed position relative to the mouthpiece pressure which, in turn, affects the driving of the oscillations in the air column of the tube resulting in a downward shift of the frequency from the resonance frequency of the tube. We have demonstrated such effects in our functional model although we experienced some difficulty in determining reed phase shifts accurately. We attempted to determine reed phase shifts by correlating the delayed mouthpiece pressure waveform with the reed position waveform for increasing amounts of delay. If t_c is the delay time which produces the maximum correlation, then the reed phase shift η is given by

$$\eta = \tan(2\pi t_c T^{-1}), \quad (12)$$

where T is the period of the mouthpiece pressure oscil-

lations. We found, however, that the delay time t_c was different for different portions of the same signals. We do not believe that this is due to any problem with the correlation method, but that the reed phase shift in our model actually does vary in time. It is not yet clear whether this also occurs in an actual clarinet. Although we determined the reed phase shifts on what appeared to be steady-state signals, it is possible that there were still some transient effects present because computational times forced us to deal with signals only a few tenths of a second after the onset of blowing.

The frequency shifts which we determined from the model did not show any variation after steady-state oscillations had apparently been achieved. They do follow the trends indicated by Backus' data. Larger average reed phase shifts and larger rest openings each produce larger frequency shifts. Computed results obtained from the model are shown in Fig. 8 where fractional frequency shift $\Delta f/f$ is plotted against average reed phase shift η for two different rest openings. The crosses joined by dashed lines in Fig. 8 show data from Backus under the assumption that double his average reed opening is equal to our rest opening. Differences between his data and our results may be attributable to a difference in the Q of the instruments involved (his instrument and our model).

D. Waveforms and spectra

A major motivation in the creation of a model of a clarinet is the study of tone production. One must then ask what kind of tones the model produces. Of course, since our model is not of a real clarinet, we cannot appropriately compare the tones from our model with those of a real clarinet. It is of interest, however, to see how the spectra of our model generated tones look.

Figure 9 shows mouthpiece and radiated pressure

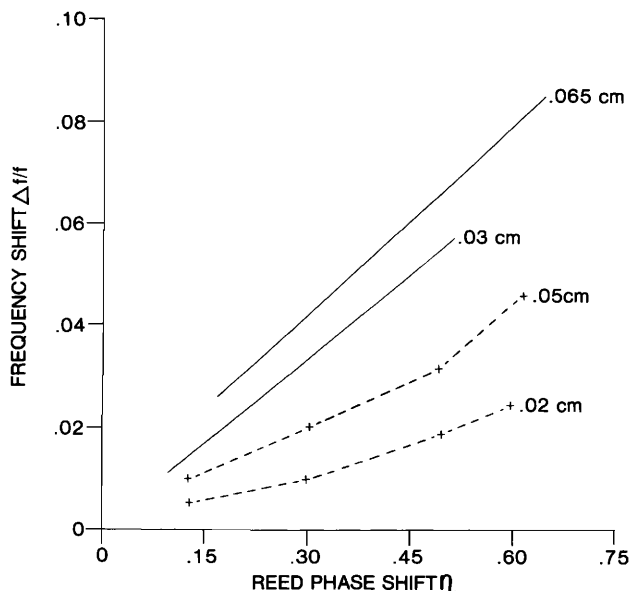


FIG. 8. Fractional frequency shift in the clarinet model (solid lines) as a function of reed phase shift for two different rest openings. Data from Backus is shown by crosses joined by dashed lines.

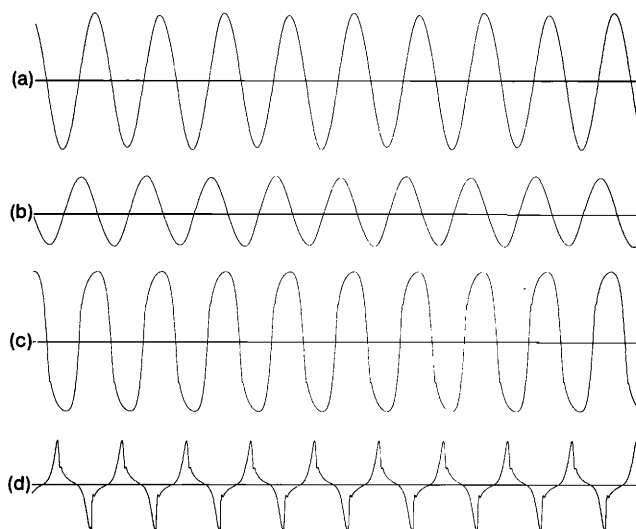


FIG. 9. Waveforms from the clarinet model: (a) mouthpiece pressure for a tone produced with "low" blowing pressure and nonbeating reed, (b) radiated pressure for the same tone, (c) mouthpiece pressure for a tone produced with "high" blowing pressure and beating reed, (d) radiated pressure for the same tone.

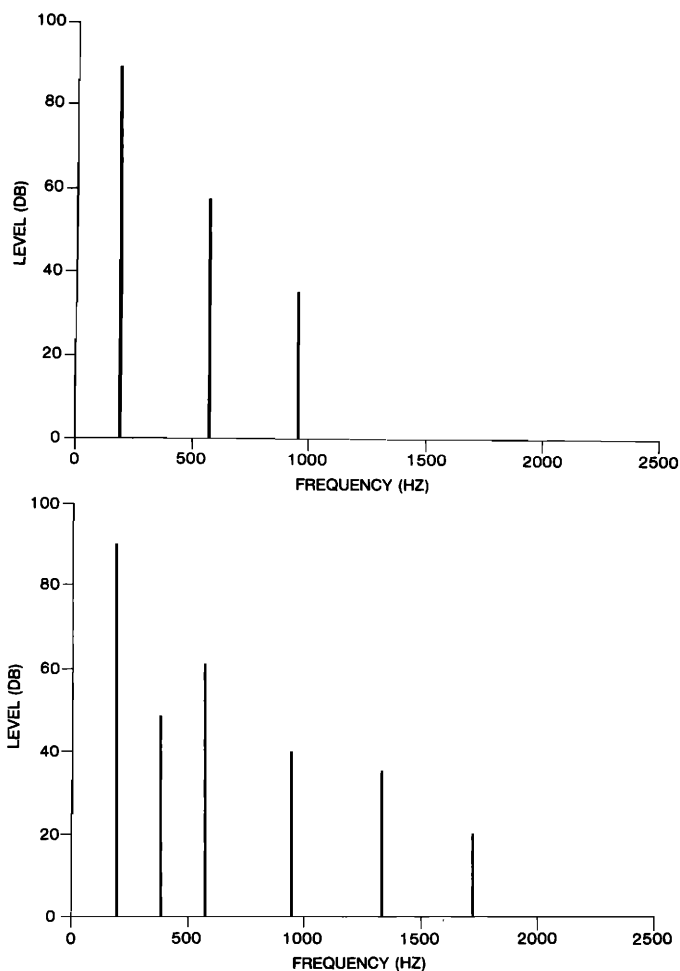


FIG. 10. Spectra of mouthpiece pressure (top) and radiated pressure (bottom) for the nonbeating reed waveforms of Fig. 9.

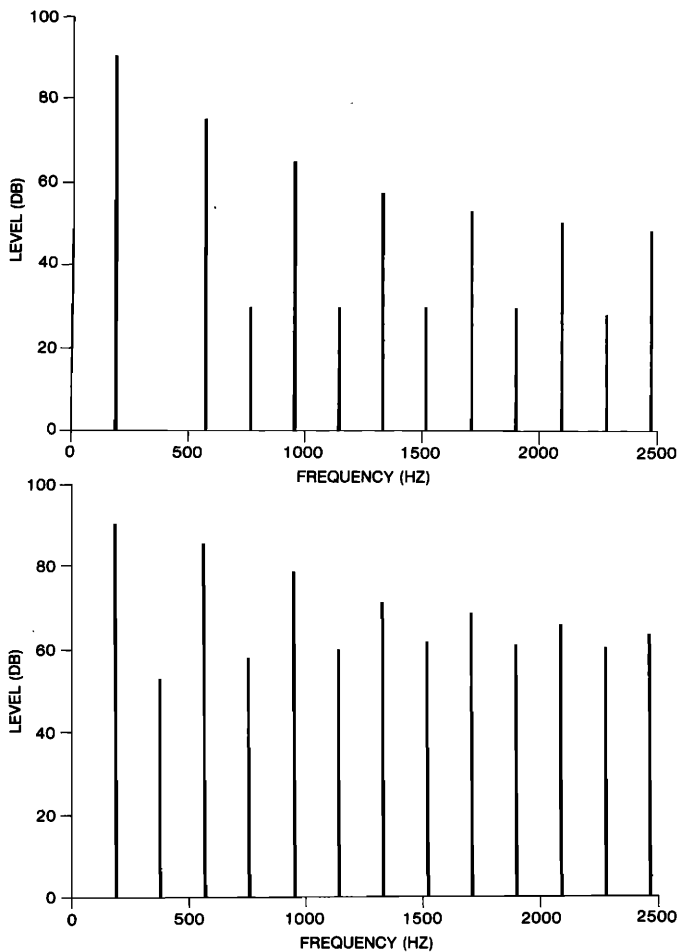


FIG. 11. Spectra of mouthpiece pressure (top) and radiated pressure (bottom) for the beating reed waveforms of Fig. 9.

waveforms from our model for a "low" blowing pressure and nonbeating reed and for a "high" blowing pressure and beating reed. The frequency of the fundamental is about 190 Hz. The relative amplitudes of the waves have no meaning since they were all scaled differently in preparing the figure. Spectra for these waves are shown in Figs. 10 and 11. Similar spectra were observed in the laboratory for the mouthpiece spectra of a simplified clarinet. In all of these spectra the power level of the fundamental was arbitrarily set at 90 dB. The relative increase of level in the higher harmonics in the radiated pressure compared to the mouthpiece pressure results from a greater radiation efficiency as frequency increases. We also see relatively higher levels in the higher harmonics (including the even harmonics) of the beating reed tone spectra due to increased nonlinear reed aperture volume flow.

The functional model will also allow us to look at transient behavior in the simplified clarinet. Figure 12

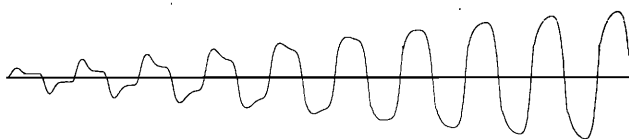


FIG. 12. Mouthpiece pressure in the clarinet model at the onset of blowing for a beating reed case.

shows a mouthpiece pressure waveform from our model at the onset of blowing in which a considerable evolution in the waveform is apparent. This waveform was produced by a blowing pressure that was turned on abruptly and so may not be entirely representative of an actual clarinet where a player would increase blowing pressure more gradually.

SUMMARY

We have argued that functional modeling can be a useful tool for understanding the physical behavior of musical systems. The results that we obtained with our model of a simplified clarinet show that it is possible to capture some rather subtle phenomena with a sufficiently detailed model. Unfortunately, we also found that such functional modeling can consume tremendous amounts of effort and computer time. It was the advent of the high-speed computer which made functional modeling possible and we expect that increased computer speed and capacity will make it more useful. Already there are computers available on which the model would run several times faster than on our present machine. Even at our present computational speed there seems to be much more that can be learned from the model.

Continued work with the current model should probably be done on the damping characteristics of the player's lip on the reed. We do not yet feel that we have handled the reed damping in a realistic manner. Also, the effect of the player's lip on the boundary conditions for the reed equation should be investigated further. Beating reed effects and transient behavior at the onset of blowing are other areas where our current model could provide more information. Possibilities also exist that the current model could be made more computationally efficient, perhaps by using different numerical procedures, and these should be considered.

When the model can be made to run faster, either by improved efficiency or by implementation on a faster computer, features which we have omitted in order to simplify the model could be added. The inclusion of frequency dependence in both the viscous and heat conduction losses could be done more correctly. The three-dimensional nature of the reed aperture, i.e., the fact that not all of the volume flow enters the mouthpiece in the first section of the tube, should eventually be included in the model. The coupling of the air vibrations to the blowing pressure is another feature which we omitted which may have some effect on tone production. And, of course, tone holes and tube flare will eventually need to be included in the model to make it more musically interesting.

ACKNOWLEDGMENTS

We are indebted to Arthur H. Benade and an anonymous reviewer for many helpful comments in the preparation of the manuscript.

APPENDIX

To derive the resistance to air flow due to viscous drag on the walls of the tube we consider a plane wall

moving arbitrarily through air. The drag force per unit area on the wall is given by

$$F = -\mu(\partial u/\partial y)_{y=0}, \quad (13)$$

where μ is the coefficient of viscosity of air, u is the particle velocity of the air relative to the wall, and y is the distance from the wall. The particle velocity is given by the diffusion equation

$$\partial^2 u/\partial y^2 = (\rho/\mu)\partial u/\partial t \quad (14)$$

subject to the boundary conditions $u(\infty, t) = 0$ and $u(0, t) = g(t)$. The solution to this equation with the given boundary conditions is

$$u = \int_0^t g(x) \frac{y}{2} \left(\frac{\rho}{\mu\pi}\right)^{1/2} (t-x)^{-3/2} \exp[-\rho y^2/4\mu(t-x)] dx, \quad (15)$$

where we have assumed that the wall is initially at rest [i.e., $g(t) = 0$ for $t < 0$]. Taking the derivative to get the drag force we obtain

$$F = \frac{-1}{2} \left(\frac{\rho\mu}{\pi}\right)^{1/2} \int_0^t g(x)(t-x)^{-3/2} \times [1 - \rho y^2/2\mu(t-x)] \exp[-\rho y^2/4\mu(t-x)] dx. \quad (16)$$

This expression must be evaluated at $y = 0$ to get the force on the wall, but y cannot be set to zero before doing the integration because of the singularity which that produces in the integrand. To investigate the properties of the integral further, consider what happens when $g(x)$ is a step function at $t = 0$ (i.e., at $t = 0$ the wall acquires a constant velocity V), then

$$F = \frac{-1}{2} V \left(\frac{\rho\mu}{\pi}\right)^{1/2} \left(\int_0^t (t-x)^{-3/2} \times [1 - \rho y^2/2\mu(t-x)] \exp[-\rho y^2/4\mu(t-x)] dx \right)_{y=0}. \quad (17)$$

Now performing the integration and letting y go to zero we get

$$F = V(\rho\mu/\pi t)^{1/2}. \quad (18)$$

Thus, the drag force on a wall which takes a step function change in velocity falls off as the inverse square root of the time since the step. Now, the numerical calculation of the volume velocities in the tube takes place at finite time intervals and the change in the volume velocity for any section of tube from one interval to the next occurs in the calculation as a step.

For a succession of step changes in the particle velocity u of the air in the tube, we write the drag force at the wall after the N th step as

$$F = (\rho\mu/\pi h)^{1/2} \sum_{n=1}^N (u_{N-n} - u_{N-n-1}) n^{-1/2}, \quad (19)$$

where h is the constant time interval between steps.

¹H. L. F. Helmholtz, *Sensations of Tone* (Peter Smith, New York, 1948).

²D. C. Miller, *The Science of Musical Sound* (McMillan, New York, 1934).

³H. Bouasse, *Instruments à Vent* (Librairie Delagrave, Paris, 1929).

⁴V. Aschoff, "Experimentelle Untersuchungen an einer Klarinette," *Akust. Z.* **1**, 77-93 (1936).

⁵C. S. McGinnis and C. Gallagher, "The Mode of Vibration of a Clarinet Reed," *J. Acoust. Soc. Am.* **12**, 529-531 (1941).

⁶P. M. Morse, *Vibration and Sound* (McGraw-Hill, New York, 1948), 2nd ed., pp. 248-253.

⁷A. H. Benade, "The Physics of Wood Winds," *Sci. Am.* **203**, 145-154 (April, 1960).

⁸A. H. Benade, "On Woodwind Instrument Bores," *J. Acoust. Soc. Am.* **31**, 137-146 (1959).

⁹A. H. Benade, "On the Mathematical Theory of Woodwind Finger Holes," *J. Acoust. Soc. Am.* **32**, 1591-1608 (1960).

¹⁰J. Backus, "Small Vibration Theory of the Clarinet," *J. Acoust. Soc. Am.* **35**, 305-313 (1963).

¹¹C. J. Nederveen, *Acoustical Aspects of Woodwind Instruments* (Frits-Knuf, Amsterdam, 1969).

¹²A. H. Benade and D. J. Gans, "Sound Production in Wind Instruments," *Ann. N. Y. Acad. Sci.* **155**, 247-263 (1968).

¹³W. E. Worman, "Self-Sustained Nonlinear Oscillations of Medium Amplitude in Clarinet-Like Systems," Ph.D. Dissertation, Case Western Reserve University, 1971.

¹⁴R. T. Schumacher, "Self-Sustained Oscillations of the Clarinet: An Integral Equation Approach," *Acustica* **40**, 298-309 (1978).

¹⁵R. T. Schumacher, "Ab initio Calculations of the Oscillations of a Clarinet," *J. Acoust. Soc. Am. Suppl.* **1**, 65, S73 (1979).

¹⁶N. H. Fletcher, "Mode Locking in Nonlinearly Excited Inharmonic Musical Oscillators," *J. Acoust. Soc. Am.* **64**, 1566-1569 (1978).

¹⁷N. H. Fletcher, "Air Flow and Sound Generation in Musical Wind Instruments," *Annu. Rev. Fluid Mech.* **11**, 123-146 (1979).

¹⁸G. A. Higbee and D. M. Turley, "Computer Model of a Pseudo-Clarinet," Brigham Young University, 1967 (unpublished).

¹⁹J. L. Flanagan and L. L. Landgraf, "Self-Oscillating Source for Vocal-Tract Synthesizers," *IEEE Trans. Audio Electroacoust.* **AU-16**, 57-64 (1968).

²⁰K. Ishizaka and J. L. Flanagan, "Synthesis of Voiced Sounds From a Two-Mass Model of the Vocal Cords," *Bell Syst. Tech. J.* **51**, 1233-1268 (1972).

²¹J. L. Flanagan, *Speech Analysis Synthesis and Perception* (Springer Verlag, New York, 1972), 2nd ed., pp. 25-35.

²²L. L. Beranek, *Acoustics* (McGraw-Hill, New York, 1954), pp. 116-128.

²³J. L. Stewart, *Circuit Analysis of Transmission Lines* (Wiley, New York, 1958).

²⁴J. Backus, "Vibrations of the Reed and the Air Column in the Clarinet," *J. Acoust. Soc. Am.* **33**, 806-809 (1961).

²⁵See for example, L. E. Kinsler and A. R. Frey, *Fundamentals of Acoustics* (Wiley, New York, 1962), 2nd ed., pp. 65-69.

²⁶W. F. Ames, *Numerical Methods for Partial Differential Equations* (Academic, New York, 1977), 2nd ed., pp. 279-281.

²⁷Jw. van den Berg, J. T. Zantema, and P. Doornenbal, Jr. "On the Air Resistance and the Bernoulli Effect in the Human Larynx," *J. Acoust. Soc. Am.* **29**, 626-631 (1957).

²⁸A. H. Benade, *Fundamentals of Musical Acoustics* (Oxford University, London, 1976).